EM Simulation of Packaged MMIC and Microstrip Antennas Using "Microwave Explorer"

Ali Sadigh, Krishnamoorthy Kottapalli, Peter Petre

Compact Software, Inc.
201 McLean Blvd.
Paterson, NJ 07504
Tel: (201) 881 1200 FAX: (201) 881 8361

ABSTRACT. A moment method solution is presented for the full-wave electromagnetics analysis of multi-layered planar structures of arbitrary shape. The mathematical formulation is based on the spectral domain integral equation and the Galerkin's testing procedure. The method is applied to shielded MMIC as well as radiating systems in the open environment. The inclusion of vertical current elements in the solution enables the method to analyze structures with vias and air bridges in both packaged and open environments. Since a periodic structure approach is used in the formulation, extension to the analysis of infinite and finite antenna arrays becomes rather straightforward. Simulated results, obtained from our electromagnetic simulator "Microwave Explorer," are presented and compared with the available data to demonstrate the versatility and the accuracy of the method. The numerical results presented include S-parameters and far field data.

I Introduction

The integral equation formulation in spectral domain has become the preferred technique for the analysis and simulation of components and discontinuities in microwave and millimeter-wave circuits and radiating systems [1]. This method is the most rigorous and efficient to perform a full-wave analysis of 3-D planar circuits. A typical 3-D planar structure is shown in Fig. 1.

We have developed an efficient and accurate numerical implementation for the analysis of passive microwave circuits and antennas based on an extension of the previous work reported in [2]. The periodic structure approach is utilized to perform efficient analysis of packaged MMIC's and interconnects. This approach has been modified and applied to structures in open environment. The modifications are such that the numerical efficiency in open environment analysis is retained, while the solution represents the results of an isolated unit cell analysis in the absence of the side walls and the top cover plate. Linear phased arrays can be easily analyzed by making use of a transformation on spectral variables.

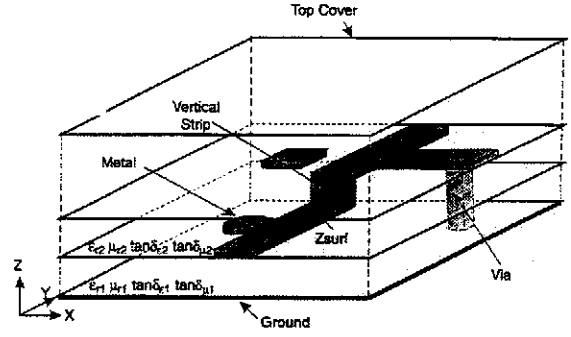

Fig. 1: A typical multi-layered 3-D structure backed by a ground plane.

The article consists of an overview of the formulation in the next section and then the simulated results. Presented simulations are intended to demonstrate sample practical problems which can be analyzed in Microwave Explorer.

II Theory

In this section, an overview of the formulation and the numerical solution which is used in Microwave Explorer is presented. Figure 1 shows a multi-layer structure in a package. The structure can consist of an arbitrary number of homogeneous dielectric layers with different parameters. Metalized traces can run in between layers or from one layer to another through vias or vertical strips. Depending on whether the circuit to be analyzed is a packaged MMIC or a radiating system such as a patch antenna, there could be conducting walls on the top, bottom, and the sides.

The dyadic spectral Green's function for a stratified medium of infinite extent is derived by using

a versatile approach in which a transmission line analogy is employed for each layer [3]-[4]. In this method, fields are decomposed into TE and TM components and the parameters of the transmission line model for each layer take on different values for each mode. This method offers versatility in computation of the Green's function of structures with arbitrary number of layers. The dielectric and magnetic losses of each layer are also included in the Green's function. This is done automatically through the lossy characteristic impedances for the transmission lines corresponding to each layer and for each TE and TM component.

The expressions for a multi-layered structure Green's function are too lengthy to include in this article. However, as an example, we assume a dielectric layer backed by a ground plane and present some of the details regarding the spectral Green's function. Assuming that there are only transverse currents present in the problem, the dyadic Green's function can be written as

$$\overline{\overline{G}}(k_x,k_y,h)=\begin{bmatrix}\hat{x}\hat{x}\,G_{xx}(k_x,k_y,h) & \hat{x}\hat{y}\,G_{xy}(k_x,k_y,h)\\ \hat{y}\hat{x}\,G_{yx}(k_x,k_y,h) & \hat{y}\hat{y}\,G_{yy}(k_x,k_y,h)\end{bmatrix} \tag{1}$$

where

$$G_{xx}=-\left(\frac{k_x^2}{k_\rho^2}Q_{TM}+\frac{k_y^2}{k_\rho^2}Q_{TE}\right) \tag{2}$$

$$G_{xy}=G_{yx}=-\frac{k_x k_y}{k_\rho^2}(Q_{TM}-Q_{TE}) \tag{3}$$

$$G_{yy}=-\left(\frac{k_y^2}{k_\rho^2}Q_{TM}+\frac{k_x^2}{k_\rho^2}Q_{TE}\right) \tag{4}$$

Here $k_\rho^2=k_x^2+k_y^2$ and k_x and k_y are the spectral variables. Q_{TM} and Q_{TE} are the equivalent TM and TE impedances seen at the dielectric junction looking into the two transmission lines representing the free space and the dielectric layer. The characteristic (wave) impedances for each region is given by

$$Z_{TM}=\frac{\eta_0 k_z}{\varepsilon_r k_0} \tag{5}$$

$$Z_{TE}=\frac{\mu_r \eta_0 k_0}{k_z} \tag{6}$$

where k_0 and η_0 are the free space wave number and impedance, respectively. ε_r and μ_r represent the relative permittivity and the permeability of the free space or the material layer. While complex ε_r and μ_r account for material losses, an imperfect conducting ground plane affects the input impedance looking into the transmission line which represents the dielectric layer.

The electric field integral equation (EFIE) formulation of the problem is given by

$$\hat{n}\times\left[\overline{E}^{s}(x,y,z)-Z_s\overline{J}(x,y,z)\right]=-\hat{n}\times\overline{E}^{i}(x,y,z) \tag{7}$$

where $\hat{n}$ is the normal vector to the metalized surfaces, $\overline{E}^{i}$ is the incident field , Z_s is the surface impedance, and $\overline{J}$ is the surface current density which can have transverse $\overline{J}_t$ and vertical J_z components. The electric field due to the surface current $\overline{E}^{s}$ is given by the integral

$$\overline{E}^{s}=\iiint\overline{\overline{G}}(x,y,z,x',y',z')\cdot\overline{J}(x',y',z')dx'dy'dz' \tag{8}$$

where $\overline{\overline{G}}$ is the dyadic Green's function for a general multi-layer structure.

Note that metalization losses are accounted for in Eq. (7). If a perfect or lossy conductor top or bottom plate or both are present, the Green's function will satisfy those boundary conditions. For packaged microwave circuits, where the circuit is enclosed in a rectangular box, the boundary conditions on the side walls are satisfied by employing a periodic structure approach.

The method of moments is utilized to solve Eq. (7) for the unknown surface electric current $\overline{J}$. The electric current in transverse direction is approximated by rooftop basis functions in the x and y directions [5]. For vertical current elements of vias and air bridges, attachment mode basis functions are employed to guarantee the continuity of the current at the junctions [2]. Applying the Galerkin's method and testing the sides of Eq. (7) results in a linear system of equations which in matrix notation is given by

$$\begin{bmatrix} \mathbf{Z}_{tt} & \mathbf{Z}_{tz} \\ \mathbf{Z}_{zt} & \mathbf{Z}_{zz} \end{bmatrix} \begin{bmatrix} \mathbf{I}_t \\ \mathbf{I}_z \end{bmatrix} = \begin{bmatrix} \mathbf{V}_t \\ \mathbf{V}_z \end{bmatrix} \qquad (9)$$

In this equation the right hand side is the excitation vector defined by port voltages and the vector on the left is the unknown current coefficients. The moment impedance matrix $\mathbf{Z}$ contains the interaction of the basis functions and is symmetric. A fast Fourier transform (FFT) algorithm is used in computing the elements of the moment matrix. This has resulted in a significant improvement in matrix fill time.

After solving Eq. (9) and obtaining the current distribution, S-parameter data is extracted by utilizing an accurate deembedding procedure which is detailed in [2]. In open environment analyses, the radiated power and far field data are computed through the use of equivalent magnetic currents on a fictitious surface above the structure [7]. Assuming that this fictitious surface in located at $z = h_0$, one can show that the far fields are related to the Fourier transform of the transverse components of the electric field by

$$E_\theta = \cos\,\phi\,\tilde{E}_x(k_x,k_y,h_0) + \sin\,\phi\,\tilde{E}_y(k_x,k_y,h_0) \qquad (10)$$

$$E_\phi = -\cos\,\theta \times [\sin\,\phi\,\tilde{E}_x(k_x,k_y,h_0) - \cos\,\phi\,\tilde{E}_y(k_x,k_y,h_0)] \qquad (11)$$

where $\tilde{}$ represents the two-dimensional Fourier transform.

An issue of prime importance in computing the moment matrix elements is the proper treatment of the poles of the spectral Green's function [6]. In the implementation of Microwave Explorer, these poles are extracted and accounted for through analytical integration in two-dimensional spectral space. The numerical results have remarkable accuracy and stability due to proper treatment of the Green's function poles.

III Simulation Results

In this section we will present simulated results for structures in packaged (MMIC) and open environments (antennas). These examples are intended to portray versatility and accuracy of Microwave Explorer. The first two circuits are analyzed using the packaged environment Green's function, i.e. inside a metallic enclosure.

Coplanar Waveguide Filter

The first circuit we shall consider is a coplanar waveguide (CPW) band reject filter as shown in Fig. 2. This filter was designed to have no transmission at 18 GHz and good transmission at 36 GHz. Air-bridges are used to equalize the potential of the two ground planes in order to eliminate the coupled slotline mode. At f = 18 GHz the stubs present short circuits, thereby allowing no transmission at this frequency. The stubs present open circuits at 36 GHz, thereby allowing good transmission.

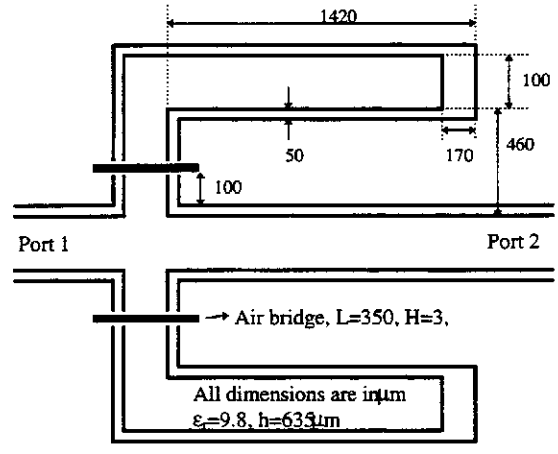

Fig. 2: The coplanar waveguide band reject filter.

Fig. 3 shows the comparison between the modeled and measured S_{11} of the CPW filter from 10-40 GHz. The results show an excellent agreement with the measured results [8]. This circuit validates the approach used to model coplanar waveguide circuits in a packaged environment. In addition, it also shows the ability of Microwave Explorer to deembed coplanar port discontinuities.

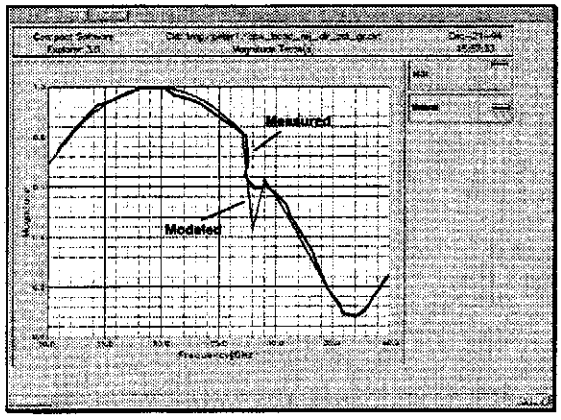

Fig. 3: Magnitude of S_{11} of the filter shown in Fig. 2.

Bandpass Filter

Figure 4 shows the layout of a bandpass filter, which is taken from the MIC Simulation Column [9]. The circuit is built on a GaAs substrate of thickness 125 μ m and dielectric constant of 12.9. The dielectric loss tangent of the substrate is 0.0005. The metal has a thickness of 4 μ m and conductivity of 4.9×10^7 Sm. The circuit has via pads of dimension 175×175 μ m with the via holes extending to the ground plane. All the physical dimensions of the filter are shown in the figure. The circuit has two ports which are terminated with 50 Ohm loads.

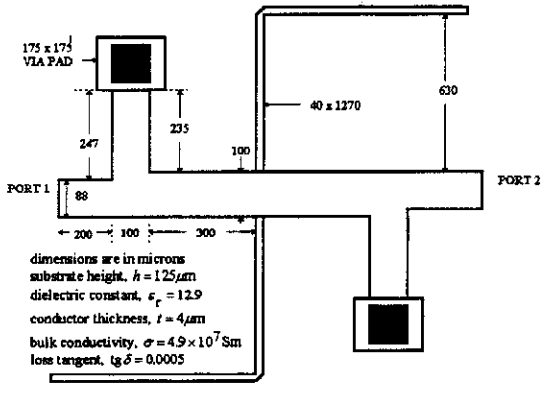

Fig. 4: The bandpass filter and its dimensions

The reflection coefficient and the transmission of the filter are plotted in Fig. 5 from 10 to 20 GHz. The response of the filter agrees well with the results of other electromagnetic simulators as reported in [10]. This circuit demonstrates the capability of Microwave Explorer to model the metal and dielectric losses accurately.

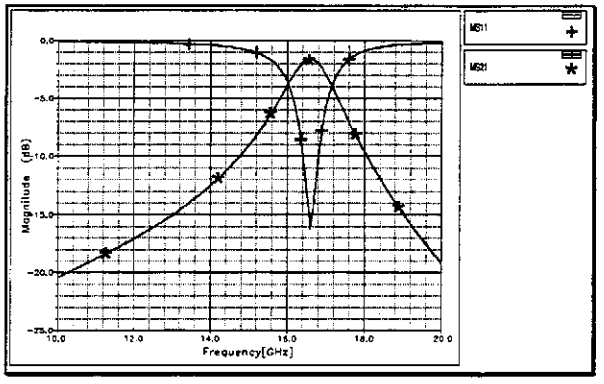

Fig. 5: Magnitude of S_{11} and S_{21} of filter shown in Fig. 4.

Patch Antenna

The rectangular microstrip patch antennas are among the most popular printed circuit antennas. In this example we consider an edge fed patch antenna whose dimensions are shown in Fig. 6. The substrate is a dielectric with ε_r=2.213 and thickness of 0.794mm. Fig. 7 shows the reflection coefficient (S_{11}) of this antenna between 5 and 20 GHz. It is observed that a good match is obtained at about 7.6 GHz due to the shorter edge being resonant. Also shown in Fig. 7 is the measured results as reported in [7]. The two results agree very well.

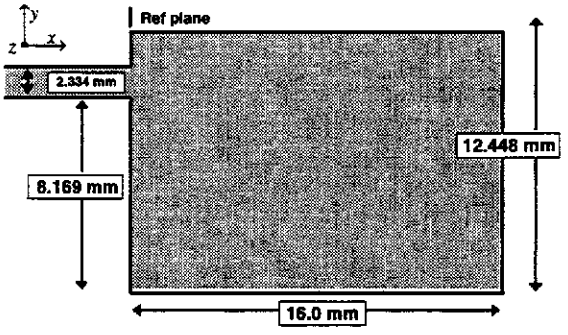

Fig. 6: Dimensions of edge-fed rectangular patch antenna

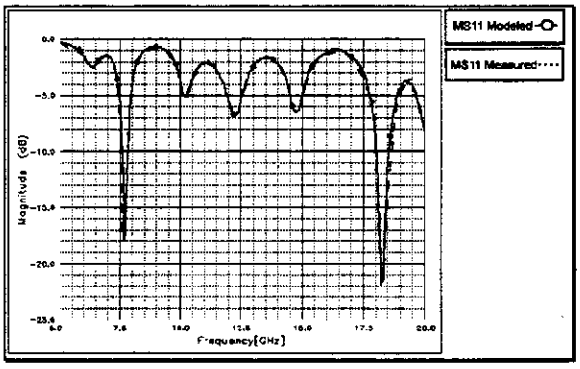

Fig. 7: Magnitude of the reflection coefficient (S_{11}) of the rectangular patch antenna of Figure 6.

The far field generated by this antenna is demonstrated in Figs. 8-a and 8-b. Note that the ripple in cross polarization in Fig. 8-a is due to the long feed line (115.6mm) used in the simulation. In fact Microwave Explorer does not need long feed lines to excite circuits. The accurate deembedding algorithm which is used in Microwave Explorer obviates the need for long feed lines. Marks ($\times$ and $+$) in Fig. 8 represent the measured data obtained from Fig. 4 of [7]. The agreement is very good. Note that in [7] the elements of the moment matrix are evaluated through direct integration. Microwave Explorer uses FFT to obtain these interactions which leads to a superior speed performance.

Figs. 8-a, 8-b: Radiation pattern of the antenna of Fig. 6 at 7.6GHz on a dB scale. Marks ($\times$ and $+$) represent the measured data [7]

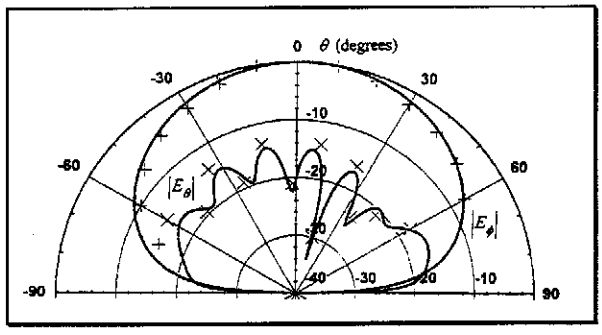

Figure 8-a. $\phi = 0^{\circ}$ cut

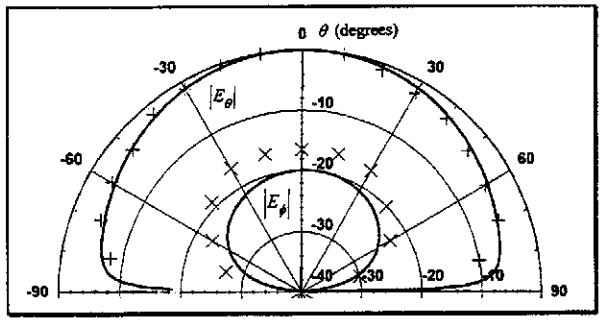

Figure 8-b. $\phi = 90^{\circ}$ cut

Four-Element Linear Array

The second example of open environment simulation is a four-element linear patch antenna array. It is made up of square patches all fed at their edges as shown in Fig. 9. The substrate which is backed by a ground plane has a thickness of 60 mils and is made of CuClad 250, with $\varepsilon_r = 2.45 \pm 0.04$.

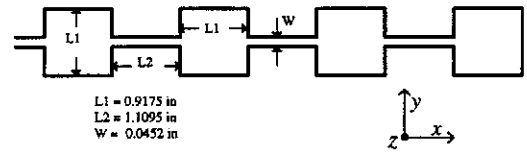

Figure 9. The four element linear patch antenna array

Antenna arrays are among problems that are considered very large and the computational cost of their simulation is usually very high. For this reason usually only one element of an array is analyzed and interactions between elements are either neglected or approximated for, e.g. [11]. In this example we analyze the entire circuit and therefore all the element interaction are automatically included in the solution.

The center frequency of the array is found to be at 3.915GHz as shown in Fig. 10. The computed far field data in E-plane ($\phi = 0^{\circ}$) at the frequency of resonance is shown in Fig. 11. Note that there is a large difference between the relative amplitudes of E_θ (solid line) and E_ϕ (broken line). During the simulation it was found that around the resonance frequency the radiation pattern was fairly insensitive to the changes in frequency. Microwave Explorer predicted a gain of almost 13dB for the array. The data presented in Figs. 10 and 11 agree very well with the measured and simulated results of Figs. 8 and 7 of [11].

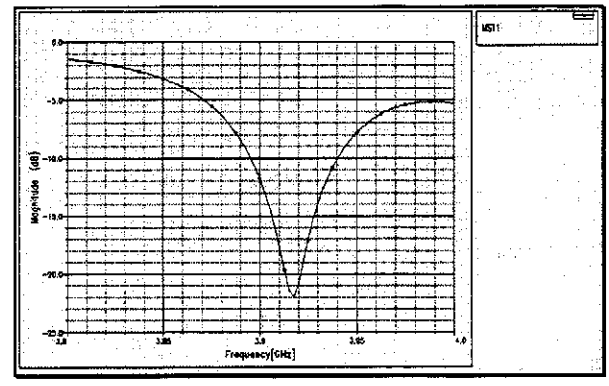

Fig. 10: Magnitude of the reflection coefficient (S_{11}) of the antenna array of Fig. 9.

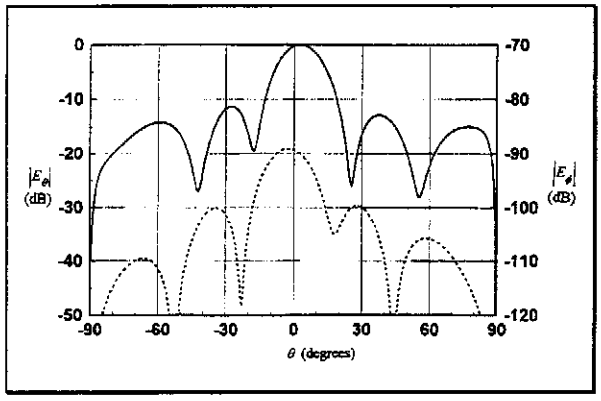

Fig. 11: Far field pattern in the *E*-plane ($\phi = 0^{\circ}$) of the antenna array of Fig. 9 at 3.915 GHz. Solid line represents the E_{θ} data and broken line the E_{ϕ}.

Two-Port Asymmetric Antenna

The structure for this two-layer problem is shown in Fig. 12. It consists of two orthogonal crossed dipoles which are electromagnetically coupled to two orthogonal microstrip lines. The length of the two dipoles are different and as a result a dual frequency operating mode is obtained. The feed lines are connected to 50 Ohm terminations.

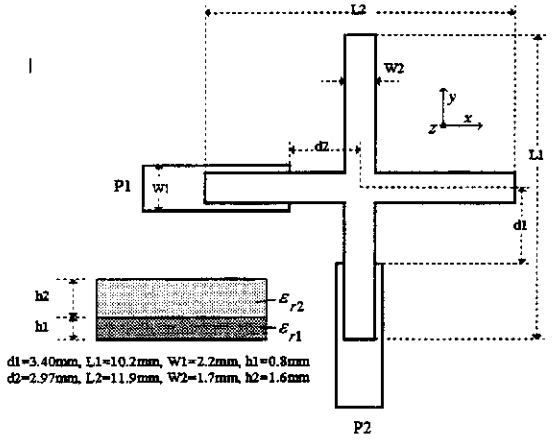

Figure 12. Dimensions of the 2-port asymmetric antenna

Fig. 13 shows the reflection coefficient of the ports (S_{11} and S_{22}) and the transmission between them (S_{12}) on a logarithmic scale. This data is in excellent agreement with the results shown in [12]. The resonant frequencies of the long dipole at 8.45 GHz and the short dipole at 9.55 GHz are within 0.5% of the values observed in [12]. As it is observed in the Figure, the incident power is largely radiated at the resonance frequencies of the dipoles and transmitted from one port to the other at 11.35 GHz.

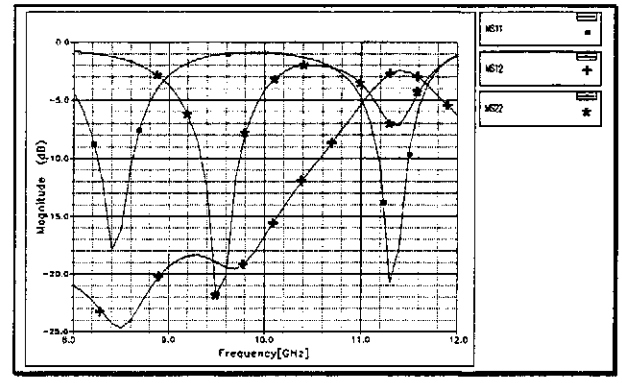

Fig. 13: Magnitude of the S-parameters of the antenna shown in Fig. 12.

The radiation pattern graphs for this structure at 8.45 GHz are presented in Figure 14. Here the first port is excited while the second one is terminated to a 50 Ohm load. Note that due to a good isolation between the ports at this frequency, the cross polarization level is low. This data also agrees favorably with the measured and calculated results in [12].

Fig. 14-a, 14-b: Radiation patterns at 8.45GHz for co- (solid line) and cross-polarization (broken line).

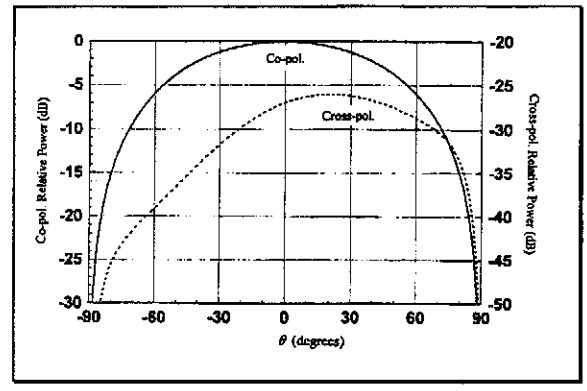

14-a) *H*-plane ($\phi = 90^{\circ}$)

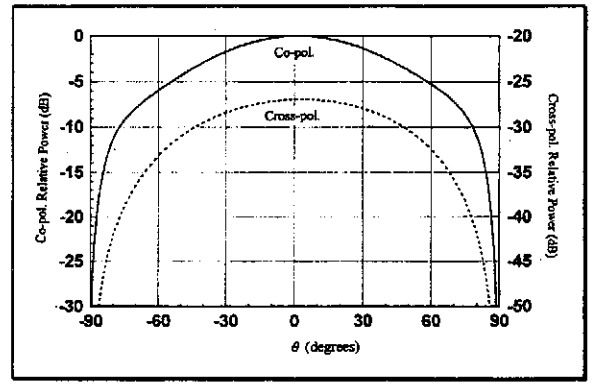

14-b) *E*-plane ($\phi = 0^{\circ}$)

IV Conclusions

The article briefly addressed the underlying theory used in the development of Compact Software's full-wave EM simulator "Microwave Explorer." The use of FFT and other numerical techniques has resulted in a significant speed enhancement in the package. Simulated results for sample microwave and antenna structures were presented which demonstrate the versatility of the numerical techniques utilized in Microwave Explorer. The accuracy of the open structure analysis and the far field calculations, which have been recently added to the simulator, were verified against the measured or other available data.

Microwave Explorer belongs to a class of simulators which are referred to as 3-D planar. It is thus optimized to only handle structures which are planar in nature with homogenous dielectric layers.

References

[1] T. Itoh, "Numerical Techniques for Microwave and Millimeter Wave Passive Structures," New York: Wiley, 1989.

[2] A. Hill, J. Burke, and K. Kottapalli, "Three Dimensional Electromagnetic Analysis of Shielded Microstrip Circuits," International Journal of Microwave and Millimeter-Wave Computer-Aided Engineering, Vol. 2, No. 4, 1992, pp. 286-296.

[3] T. Itoh, "Spectral Domain Immitance Approach for Dispersion Characteristics of Generalized Printed Transmission Lines," IEEE Transactions on Microwave Theory and Techniques, Vol. MTT-28, No. 7, July 1980, pp. 733-736.

[4] S.G. Pan, and I. Wolff, "Scalarization of Dyadic Spectral Green's Functions and Network Formalism for Three-Dimensional Full-Wave Analysis of Planar Lines and Antennas," IEEE Transactions on Microwave Theory and Techniques, Vol. 42, No. 11, Nov. 1994, pp. 2118-2127.

[5] R.W. Jackson, "Full-Wave, Finite Element Analysis of Irregular Microstrip Discontinuities," IEEE Transactions on Microwave Theory and Techniques, Vol. 37, No. 1, pp. 81-89.

[6] F.J. Demuynck, G.A.E. Vanderbosch, and A.R. Van de Capelle, "Analytical Treatment of the Green's Function Singularities in a Stratified Dielectric Medium," Proceedings of the European Microwave Conference 1993, Madrid, Spain, September 1993, pp. 1000-1001.

[7] S.C. Wu, N.G. Alexopoulos, and O. Fordham, "Feeding Structure Contribution to Radiation by Patch Antennas with Rectangular Boundaries," IEEE Transactions on Antennas and Propagation, Vol. 40, No. 10, October 1992, pp. 1245-1249.

[8] Amjad. A. Omar, Y. Leonard Chow, "A solution of Coplanar Waveguide with Air-Bridges using Complex Images", IEEE Transactions on Microwave Theory and Techniques, Vol. 40, No. 11, Nov. 1992, pp. 2070-2077.

[9] MIC Simulation Column, International Journal of Microwave and Millimeter-Wave Computer-Aided Engineering, Vol. 4, No. 2, April 1994, pp. 203-212.

[10] MIC Simulation Column, International Journal of Microwave and Millimeter-Wave Computer-Aided Engineering, Vol. 4, No. 4, October 1994, pp. 411-431.

[11] H.Y.D. Yang, C.H. Chen, J.A. Castaneda, and W.C. Wong, "Design of Microstrip Line-Fed Patch Arrays Including Mutual Coupling," International Journal of Microwave and Millimeter-Wave Computer-Aided Engineering, Vol. 4, No. 1, 1994, pp. 31-42.

[12] R. Gillard, J.H. Corre, M. Drissi, and J. Citerne, "A General Treatment of Matched Terminations Using Integral Equation Modeling and Applications," IEEE Transactions on Microwave Theory and Techniques, Vol. 42, No. 12, Dec. 1994, pp. 2545-2553.